A novel human monogenic obesity trait: severe early-onset childhood obesity caused by aberrant expression of agouti-signaling protein (ASIP): a case report

Antje Körner (antje.koerner@medizin.uni-leipzig.de)
Center for Pediatric Research Leipzig (CPL), University Hospital for Children & Adolescents, University of Leipzig, Leipzig https://orcid.org/0000-0001-6001-0356

Elena Kempf
University of Leipzig, Medical Faculty, University Hospital for Children and Adolescents, Center for Pediatric Research, Leipzig, Germany

Robert Stein
University of Leipzig, Medical Faculty, University Hospital for Children and Adolescents, Center for Pediatric Research, Leipzig, Germany

Martha Hanschkow
University of Leipzig, Medical Faculty, University Hospital for Children and Adolescents, Center for Pediatric Research, Leipzig, Germany

Anja Hilbert
University of Leipzig, Medical Faculty, Department of Psychosomatic Medicine and Psychotherapy, Leipzig, Germany

Rami Abou Jamra
University Medical Center Leipzig https://orcid.org/0000-0002-1542-1399

Andreas Kühnapfel
University of Leipzig, Medical Faculty, Institute for Medical Informatics, Statistics and Epidemiology, Leipzig, Germany

Yu-Hua Tseng
Joslin Diabetes Center/Harvard Medical School https://orcid.org/0000-0003-2053-9559

Claudia Stäubert
Rudolf Schönheimer Institute of Biochemistry, Faculty of Medicine, Leipzig University, Johannisallee 30, 04103, Leipzig, Germany https://orcid.org/0000-0003-0721-8507

Torsten Schöneberg
Rudolf Schönheimer Institute of Biochemistry, Faculty of Medicine, Leipzig University, Johannisallee 30, 04103, Leipzig, Germany

Peter Kuhnen

Charité – Universitätsmedizin Berlin, corporate member of Freie Universität Berlin, Humboldt-Universität zu Berlin, and Berlin Institute of Health https://orcid.org/0000-0003-0211-176X

William Rayner

Helmholtz Zentrum München - German Research Center for Environmental Health, Institute of Translational Genomics, Neuherberg, Germany

Eleftheria Zeggini

Institute of Translational Genomics, Helmholtz Zentrum München https://orcid.org/0000-0003-4238-659X

Wieland Kiess

University of Leipzig

Matthias Blüher

Leipzig University https://orcid.org/0000-0003-0208-2065

Kathrin Landgraf

Center for Pediatric Research Leipzig (CPL), University Hospital for Children & Adolescents, University of Leipzig, Leipzig

---

Article

Keywords: Early-onset obesity, hyperinsulinemia, red hair color, agouti signaling protein (ASIP), agouti, case report

Posted Date: March 21st, 2022

DOI: https://doi.org/10.21203/rs.3.rs-1459517/v1

Version of Record: A version of this preprint was published at Nature Metabolism on December 19th, 2022. See the published version at https://doi.org/10.1038/s42255-022-00703-9.

Abstract

In a patient with extreme childhood obesity, we identified a heterozygous tandem duplication at the *ASIP* (agouti-signaling protein) gene locus causing ubiquitous, ectopic *ASIP* expression. The mutation places *ASIP* under control of the ubiquitously active itchy E3 ubiquitin protein ligase (*ITCH)* promoter, driving the ubiquitous generation of ASIP as evidenced in patient-derived induced pluripotent stemm cells for all germ layers. The patient´s phenotype of early-onset obesity, overgrowth, red hair, and hyperinsulinemia is concordant with that of mutant mice ubiquitously expressing the homolog *agouti*. ASIP represses melanocyte-stimulating hormone-mediated activation of as an inverse agonist of the melanocortin receptors, thereby affecting eating behavior, energy expenditure, adipocyte differentiation, and pigmentation, as observed in the index patient. Furthermore, we identified another patient with the identical mutation, ectopic *ASIP* expression and a similar phenotype. Thus, human obesity caused by ubiquitous *ASIP* expression is a novel monogenic trait, potentially treatable by melanocortin receptor agonists.

Full Text

Although there is doubtless a genetic component of common obesity, monogenic forms of human obesity are very rare.[1] Most of these single-gene defects affect the leptin-melanocortin 4 receptor (MC4R) pathway, which centrally regulates food intake and energy balance.[2,3] Detection of these[4] and new monogenic obesity traits[5] will not only improve our understanding of obesity mechanisms but guide the development of novel targeted pharmacotherapies increasingly available for affected patients.[6]

In a bottom-up approach derived from functional studies with patient-derived adipocytes, we identified a novel monogenic trait of early-onset extreme obesity.

Case Report

A girl of non-consanguineous parents of European ancestry first presented at the age of 1.9 years with overgrowth and severe obesity. From infancy onwards, she was reported to have a constant desire for food and developed progressive extreme obesity and tall stature (Fig. 1A + B) accompanied by first signs of hepatic steatosis and severe hyperinsulinemia in early childhood (Fig. 1C + D; Supplementary Appendix, Figure S1). Both parents also suffer from obesity (Fig. 1E). The father has type 2 diabetes, hypertension, and gout. In distinct phenotypic features (red hair color, pale skin, freckles), the girl resembles her father. Clinically relevant variants in genes related to monogenic obesity and other inherited diseases were excluded by exome sequencing. At the age of 12.4 years, with BMI of 47.6 kg/m² (BMI SDS: 3.8, weight: 156 kg, height: 181 cm, 3.34 SDS), she underwent sleeve gastrectomy leading to weight loss of 40 kg but subsequently regained weight (Fig. 1B-D; Supplementary Appendix, Figure S1).

Results

Identification of ectopic ASIP expression in adipose tissue

We obtained a subcutaneous adipose tissue (AT) sample from the patient during bariatric surgery. Considering the severe overgrowth and obesity, we hypothesized that the AT-derived stromal vascular fraction (SVF) cells showed alterations in proliferative and/or adipogenic capacity. Proliferation of the patient's SVF cells was not enhanced compared to SVF cells from four age-matched controls with obesity (Supplementary Appendix, Table S1; Supplementary Appendix, Figure S2). However, the patient's cells showed increased adipocyte differentiation, even in long-term cultivation (Fig. 2A–D). We further found reduced mitochondrial maximum respiration, spare capacity, and proton leak in the patient's SVF cells as proxies for reduced energy expenditure (Fig. 2E).

To identify potential molecular causes for the enhanced adipogenesis, we searched for differentially expressed genes in the patient's SVF cells through transcriptome-wide analyses. One single gene encoding agouti-signaling protein (*ASIP*) was highly overexpressed in the index patient´s cells (Fig. 2F).

We confirmed ectopic *ASIP* expression in several cell types, including isolated adipocytes and peripheral blood leukocytes, indicating ubiquitous expression in the patient (Fig. 2G–I). Concordant with the GTEx catalogue, we found high *ASIP* gene expression in skin and low expression in other normal human tissues (Supplementary Appendix, Figure S3). In the patient's cells, we found ectopic ASIP protein in SVF cell lysates and conditioned medium, and inhibition of the secretory pathway leading to retention of ASIP, confirming that the ectopically expressed ASIP is secreted[7] (Fig. 2J).

Physiologically, *ASIP* is expressed in the skin and regulates hair pigmentation through interaction with the melanocortin-1 receptor (MC1R). Ubiquitous expression of the murine *ASIP* homolog *agouti* in mice leads to yellow fur and obesity due to increased food intake, lipid storage in AT, and reduced energy expenditure.[8–11] Hence, the concordant phenotype associated with ectopic expression of *ASIP* in our subjects is a novel monogenic obesity trait in humans.

Chromosomal rearrangement generating an ITCH-ASIP fusion transcript as cause of ubiquitous ASIP expression

Based on our finding of ectopic *ASIP* expression in the patient, we hypothesized an *ASIP* gene locus alteration. Genetic analyses including trio whole genome sequencing (WGS), screen for copy number variation (CNV), and cloning of the breakpoint sequence revealed a heterozygous 183-kbp tandem duplication on chromosome 20 encompassing the genes *ASIP*, *AHCY* (adenosylhomocysteinase), and *ITCH* (itchy E3 ubiquitin protein ligase) (Fig. 3A).

Our index patient inherited the mutation from her father, as evidenced by ectopic *ASIP* expression in his peripheral blood leukocytes (Fig. 3B) and the presence of the duplication-specific *ITCH-ASIP* breakpoint sequence confirmed by WGS and breakpoint-specific qPCR (Fig. 3C).

By 5'-RACE-PCR and RNA-sequencing from peripheral blood and SVF cells, we demonstrated that the genetic rearrangement creates an *ITCH-ASIP* transcript consisting of the first two non-coding *ITCH* exons (5'-UTR) fused to the *ASIP* coding exons (Fig. 3D). This indicates that *ASIP* expression is under the control of the *ITCH* promoter. Since *ITCH* is ubiquitously expressed in human tissues (Fig. 3E and concordant with the GTEx catalogue), it explains the ubiquitous expression of *ASIP* in our patient.

We verified functional *ITCH-ASIP* interaction in luciferase reporter assays showing that a 2.8-kbp genomic region located upstream of *ITCH* exon 1 is capable of driving gene expression (Fig. 3F). Furthermore, we generated an artificial fusion gene by cloning the *ITCH-ASIP* fusion cDNA sequence under control of the 2.8-kbp *ITCH* promoter and confirmed increased production and secretion of ASIP protein (Fig. 3G) independent of the presence or absence of the *ITCH* 5'-UTR (Fig. 3H).

Thus, the chromosomal rearrangement positioning *ASIP* under the control of the *ITCH* promoter is the cause of the ubiquitous expression of *ASIP* in our patient.

ASIP **is ubiquitously expressed in cells of all three germ layers generated from patient-derived iPSCs**

In order to prove ubiquitous *ASIP* expression due to the genetic rearrangement in cells of the patient, we generated induced pluripotent stem cells (iPSCs) from patient-derived SVF cells and two control children, and subsequently differentiated them into cells of the three germ layers mesoderm, ectoderm and endoderm. We show that in iPSCs from the patient compared to the controls, ectopic *ASIP* expression persists (Fig. 4A) and ASIP protein is secreted into the supernatant (Fig. 4B). In addition, we observed that ectopic *ASIP* expression is present in patient-derived iPSCs compared to controls after differentiation in all germ layers (Fig. 4C).

We further performed cAMP accumulation assays in transiently with human MC1R or MC4R transfected CHO-K1 cells, to experimentally show that ASIP indeed acts as inverse agonist not only at MC1R but also at MC4R (Fig. 4D). We found that in absence of the agonist, increasing concentrations of ASIP cause a reduction of basal activity of both human MC1R and MC4R activity with IC_{50} values of 4.4 nM and 16.9 nM, respectively. As expected α-MSH exhibits agonistic activity at both receptors (MC1R: EC_{50} = 2.3 nM; MC4R: EC_{50} = 10.6 nM), but presence of 100 nM ASIP causes a reduction of α-MSH potency at both receptors, MC1R (EC_{50} = 65 nM) and MC4R (EC_{50} = 149 nM).

Hence, ubiquitous expression of *ASIP* is detectable in patient-derived cells of all three germ layers supporting the hypothesis that ectopic ASIP might affect processes related to eating behaviour and energy expenditure due to its antagonistic effect on the MC4R in the hypothalamus of our patient.

Phenotypic characterization of the index patient

Considering the similar phenotype with respect to hair color and obesity in mouse models ubiquitously expressing the murine homolog *agouti*, we performed more detailed phenotypic characterization of the patient.

During childhood, the patient reported being continuously hungry, except after eating very large amounts of food. She tried consciously to control food intake. At the age of 16, she scored high on the Eating Disorder Examination-Questionnaire and the Dutch Eating Behavior Questionnaire, showing high cognitive restraint (> 85th percentile) as well as extreme eating, weight, and shape concern (> 95th percentile). She did not report binge eating, external (< 5th percentile) or emotional eating (< 25th percentile).

A clinical-psychological exploration noted remarkably low physical activity. Furthermore, indirect calorimetry revealed a reduced resting metabolic rate (1,660 kcal/day, accounting for only 77.4% of the expected), further underlining her reduced energy expenditure.

The father, harboring the same chromosomal rearrangement, had been taller and heavier than his peers from birth onwards. Starting at the age of 10 years, he engaged in professional athletic sports and lost some weight. Nonetheless, he reported weighing 125 kg at the age of 18 years (BMI 36 kg/m²). He did not, however, score conspicuously on eating questionnaires at the age of 52 years.

Both the patient and her father have red hair color and pale skin with freckles (Fig. 1E), which is another characteristic concordant with the yellow fur of the mice ectopically expressing *agouti* and is due to the action of agouti as an inverse agonist at the melanocortin-1 receptor in the skin. We confirmed that neither carries any genetic variant known to be associated with red hair, for example in *MC1R*[12] (Supplementary Appendix, Table S2).

Hence, overall the *ASIP* mutation is likely to be responsible for the clinical phenotype of our patient with early onset extreme obesity, altered eating behavior, reduced energy expenditure, and hypopigmentation.

Screening for additional patients with ASIP mutations

The type of genetic rearrangement is not readily detectable by standard genetic screening focusing on single nucleotide variations, which may explain why there are as yet no cases with detected *ASIP* mutations in the UK Biobank subset with available exome sequencing information.

We targetedly screened 20 patients with a phenotype indicative of defects in the POMC pathway (extreme obesity, red hair color) originally suspected but not diagnosed for *POMC*-deficiency, for *ASIP* mutations, however could not identify a patient with a similar *ITCH-ASIP* fusion (Figure S4).

By re-evaluation of available exome sequencing data of children from our obesity clinic, we identified another girl with the identical 5´*ITCH-ASIP* fusion as confirmed by WGS and breakpoint-specific qPCR, and, importantly, also an ectopic *ASIP* expression in peripheral blood leukocytes (Figure S4).

The identified girl has red hair, fair skin, severe early-onset obesity and tall stature (BMI 20.85 kg/m², BMI SDS 2.65, height 109.5 cm, height SDS 1.74 at the age of 3.8 years) despite normal birth weight and height. The girl was otherwise healthy with age-appropriate psychomotor development. Her parents reported her suffering from severe hyperphagia from birth onwards, with satiety lasting no longer than 2

hours, stealing of food and rage attacks when food was refused. The parents restricted food intake and sweets tightly aiming to prevent even more weight gain.

Identification of the second, unrelated patient holds promise of detecting more patients with ubiquitous *ASIP* expression if genetic diagnostic is extended to chromosomal rearrangements.

Discussion

We report a novel human monogenic obesity trait that presents with extreme early onset obesity, accelerated linear growth beyond what would be expected for children with obesity,[13] and hypopigmentation. In a bottom-up approach based on experimental data, we identified ubiquitous *ASIP* expression due to chromosomal rearrangement as the cause of the phenotype. The identified tandem duplication leads to the generation of an ectopically expressed *ITCH-ASIP* fusion mRNA under control of the ubiquitously expressed *ITCH* promoter and results in increased levels of secreted ASIP protein. Ectopic *ASIP* expression was found in several cell types of the patient. Furthermore, patient-derived iPSCs differentiated into cells of all germ layers maintained ectopic *ASIP* expression. These findings together with the fact that *ITCH* expression was detected in the brain and hypothalamus and that ASIP acts as an inverse agonist at the MC1R and MC4R, confirm that *ASIP* may be ectopically expressed in the hypothalamus of the patient, where it can inhibit melanocortin receptors, specifically MC4R, inducing obesity.

The murine *ASIP* homolog *agouti* is well known to be linked to obesity in mice. The coding region of the human *ASIP* gene is 85% homologous to the mouse gene[14] and there is high functional conservation.[15] Concordant with our patient, several mouse models with ubiquitous expression of *agouti* develop increased body length, yellow fur, obesity, and metabolic alterations such as hyperinsulinemia.[9–11] Interestingly, similar to that in naturally occurring agouti mice,[9] ectopic *ASIP* expression in our patient is caused by a gene rearrangement resulting in a change in promoter usage and hence ubiquitous and ectopic *ASIP* expression.

Physiologically, *ASIP*/*agouti* is expressed in hair follicles and antagonizes MC1R function on hair melanocytes, and its ectopic expression is hence causing the red hair in the patient and the yellow fur in mice. The obesity phenotype is explained by agouti and ASIP sharing structural similarity with agouti-related peptide (AGRP).[16] When ectopically expressed in the hypothalamus, agouti and ASIP can interfere with the leptin-melanocortin axis by competitively antagonizing α-melanocyte-stimulating hormone at the MC4R and thereby centrally regulating food intake. However, ubiquitous *agouti* expression in mice has been reported to result in rather moderate hyperphagia compared with leptin- or leptin receptor-deficient mice.[11] Similarly, our patient reported struggling with satiety before bariatric surgery and showed restrained eating, indicating conscious counteracting against the hyperphagic drives that she herself sensed. Increased levels of incretins after bariatric surgery may affect neuronal MC4R signaling in the patient, further facilitating restrained eating.[17]

Besides hyperphagia, other mechanisms may affect the development of obesity.[11,18] AGRP in the hypothalamus affects energy expenditure,[19] locomotor activity,[20] and sympathetic tone as well as shifting substrate utilization[21] in peripheral tissues. Agouti/ASIP may have analogous effects. Indeed, we observed in our patient reduced urge for physical activity and measured a decreased resting metabolic rate at the whole body and cellular level, which might at least partially contribute to the obesity phenotype. The father suffers from obesity, diabetes, and has red hair. In childhood and adolescence he engaged intensely in competitive sports, which affects energy balance beneficially, but did not prevent obesity. Variable phenotype-genotype concordance is also known in other monogenic obesity traits, e.g. MC4R[22].

Although ectopic agouti/ASIP likely promotes obesity primarily via central effects, ectopic agouti/ASIP may also contribute to obesity through peripheral effects as described for enhanced insulin secretion in the pancreas, leptin secretion from adipocytes, reduced lipolytic activity in adipocytes, or regulation of adipogenic transcription factors,[18,23] and it may even affect activation of brown AT.[24] In line with this, the patient showed hyperinsulinemia and her SVF cells differentiated better into adipocytes than SVF cells from controls, indicating additional peripheral obesity-related effects of ubiquitous *ASIP* expression.

Likely there are more patients with undiagnosed ectopic *ASIP* expression, as the locus around *ASIP* is susceptible to genetic rearrangements.[25] Gain-of-function mutations have been described in several species,[9,26,27] and similar duplications resulting in an *ITCH-ASIP* fusion gene have been observed in sheep[28] and in quail.[29] The chromosomal rearrangement is, however, not readily detectable by routine sequencing approaches but requires techniques identifying copy number variants. Only by targeted re-evaluation we were able to find a second (unrelated) patient carrying the same genomic rearrangement as our index patient and also suffering from obesity. That this patient also shows an ectopic *ASIP* expression in blood cells further supports the finding of the tandem duplication causing the ectopic *ASIP* expression and the obese phenotype. The screening of more patients to specify the phenotype of this novel monogenic trait of ectopic *ASIP* expression is pertinent, particularly as treatment with MC4R agonists, as recently approved for deficiencies in components of the leptin-melanocortin signaling pathway,[6] provides a promising treatment option for these patients.

In summary, we provide evidence for a genomic rearrangement leading to ubiquitous expression of *ASIP* in a patient with severe early-onset obesity and overgrowth. This phenotype is concordant with mouse obesity models ectopically expressing the homolog *agouti*. Both agouti and ASIP interact with the melanocortin receptor pathways, which likely explains the obese phenotypes.

Online Methods

Oversight

The index patient and children of the control group were participants in the Leipzig Adipose Tissue Childhood[30] (NCT02208141) and the Leipzig Obesity Childhood (NCT04491344) cohorts[13]. Children and guardians provided informed consent. The studies were approved by the Ethics Committee of the University of Leipzig (265/08, 007/04).

Clinical data, evaluation of eating behavior and energy expenditure

Height was measured to the nearest of one millimeter using a rigid stadiometer. Weight was measured in underwear to the nearest of 0.1 kg using a calibrated scale. BMI and height were referenced to sex and age according to current guidelines[31] and are given as standard deviation scores (SDS). Children were categorized into overweight (1·28 < BMI SDS ≤ 1·88) or obese (BMI SDS > 1.88) as recommended by the German Working Group for Pediatric Obesity Consensus Guideline[32].

Blood parameters were measured by standard laboratory procedures in the Institute of Laboratory Medicine of the University of Leipzig, Germany.

Eating behavior was assessed by self-reports using validated questionnaires. The Eating Disorder Examination-Questionnaire (EDE-Q)[33,34] was used to assess eating disorder psychopathology regarding the subscales restraint, eating concern, weight concern, shape concern, and behavioral features such as binge-eating episodes. Scores from the patient were compared to a reference population of 1,354 women younger than 44 years of age[35]. Scores from the father were compared to a reference population of 1,166 men between 44–64 years of age[35].

The Dutch Eating Behavior Questionnaire (DEBQ)[36] evaluates emotional eating, external eating and restraint using sum scores from Likert scales. Results from the patient were compared to a reference population of 1,394 women between 14–94 years of age[36].

Resting energy expenditure of the patient was examined at the age of 15 years following an overnight fast using an indirect calorimeter (Quark RMR, Cosmed Germany) according to the manufacturer's protocol and expected metabolic rate was calculated according to her age, sex, height, and body mass.

Isolation and cultivation of SVF cells from adipose tissue

Subcutaneous adipose tissue (AT) samples were obtained from children undergoing bariatric or elective orthopedic surgery as previously described[30,37]. Briefly, AT was washed in phosphate-buffered saline (PBS) (Invitrogen) and minced. Adipocytes and stromal vascular fraction (SVF) cells were separated by digestion with a final concentration of 250 units/mL collagenase IV (Sigma-Aldrich) with subsequent processing through a nylon mesh with 400 µm pore size to remove connective tissue and centrifugation (800 x g, 5 min). Isolated adipocytes and a part of the SVF were frozen in liquid nitrogen for later RNA isolation. The remaining SVF pellet was re-suspended in PBS and filtered through a nylon mesh with 30 µm pore size and centrifuged again. Remaining erythrocytes were removed by incubation of the SVF cells

in erythrocyte lysis buffer (0.154 M NH_4Cl (Sigma-Aldrich), 0.01 M $KHCO_3$ (Merck KGaA), 0.1 mM EDTA (Sigma-Aldrich)). SVF cells were frozen in liquid nitrogen in Dulbecco's Modified Eagle Medium/Ham F-12 culture medium (DMEM/F-12) (Life Technologies, Karlsruhe, Germany) medium containing 10% fetal bovine serum (FBS) (Biochrom GmbH) and 10% dimethyl sulfoxide (Sigma-Aldrich). Cells were thawed and 24 h after seeding cells were washed three times with PBS to select for adipocyte precursor cells via plastic adherence. Isolated SVF cells were cultivated in DMEM/Ham F-12 culture medium containing 10% FBS and 100 units penicillin and 0.1 mg/mL streptomycin (Sigma-Aldrich) at 37°C and 5% CO_2 and passaged every 3–4 days.

Proliferation assay

For assessing proliferation and cell viability, 500 SVF cells were seeded at day 49, 71, and 89 of cultivation per well in 96-well plates in 5 replicates and cultivated for 8 days. After 1 and 8 days cell viability was assessed by WST-1 assay (Roche, Applied Bioscience) according to the manufacturer's protocol. Absorbance was measured 4 hours after addition of the WST-1 reagent. Afterwards, cells were fixed, stained with Hoechst 33342 (Sigma Aldrich, St. Louis, MO, USA) and counted using the BZ-8000 microscope (Keyence, Neu-Isenburg, Germany). Doubling time between d1 and d8 was calculated using the following formula[38]:

Doubling time (days) = (duration (8 days) * $\log_{10}(2)$) / ($\log_{10}$ (cell number per image d1) – $\log_{10}$(cell number per image d8)).

Differentiation assay

For assessing adipogenic capacity, 30,000 SVF cells at day 34, 49, 71, and 89 of cultivation were seeded per well in a 48-well dish. Cells were grown to confluence for 24 to 48 hours and differentiated according to the Poietics human adipose-derived stem cell–adipogenesis protocol (Lonza) for 8 days. Differentiated cells were fixed with Roti®-Histofix 4% (Carl Roth GmbH, Karlsruhe, Deutschland), double-stained with 10 µg/mL Nile red (Sigma Aldrich, St. Louis, MO, USA) and 40 µg/mL Hoechst 33342 (Sigma Aldrich, St. Louis, MO, USA), and analyzed using the BZ-8000 microscope (Keyence, Neu-Isenburg, Germany). The percentage of differentiated cells was calculated from the number of counted differentiated cells divided by the total number of cells within an image for a total of three images per cell line. A cell was defined to be differentiated when containing at least two lipid droplets. Additionally, the cells were stained with Oil Red O (Sigma Aldrich, St. Louis, MO, USA) solution (0.3% in 60% isopropanol) for 15 minutes and washed with H_2O. Oil Red O was extracted with isopropanol and absorption was measured at 540 nm.

Bioenergetic profiling

Mitochondrial function was assessed using the Seahorse XFe24 Analyzer (Agilent Technologies) and the XF Cell Mito Stress Test Kit (Agilent Technologies) using concentrations of 2 µM oligomycin, 3 µM carbonyl cyanide-4 (trifluoromethoxy) phenylhydrazone (FCCP) and 1 µM rotenone/antimycin A. In this assay oxygen consumption rate of cells is measured on basal condition after injection of oligomycin (inhibitor of the ATP synthase), after injection of FCCP (uncoupling agent disrupting the mitochondrial

membrane chain) leading to uninhibited electron flow through the electron transport chain so that the oxygen consumption reaches the maximum and after injection of rotenone and antimycin A, which fully shut down mitochondrial respiration. 15,000 SVF cells from the patient or control children were seeded into gelatine-coated wells of XFe24-plates in 3–4 technical replicates. Measurements were performed 48 hours post-transfection using XF Base Medium (Agilent Technologies) containing 2 mM pyruvate (Sigma Aldrich), 10 mM glucose (Sigma Aldrich) and 2 mM glutamine (Sigma Aldrich). Results were normalized to total protein/per well (µg) by lysing the cells in 30 µL 50 mM NaCl solution (Carl Roth) with subsequent protein quantification using the Pierce™ BCA Protein Assay Kit (Thermo Fisher Scientific).

Isolation of nucleic acids

RNA was isolated from SVF cells and reverse-transcribed as previously described[39]. From blood, RNA was extracted using the PAXgene® Blood RNA Tubes protocol (PreAnalytics). RNA from different human tissues pooled from several individuals were obtained from Clontech-Takara Bio (Saint-Germain-en-Laye, France). Genomic DNA was extracted from EDTA blood samples using the QIAamp DNA Blood Mini Kit (Qiagen GmbH).

Transcriptome-wide analyses

Gene expression was measured using a HumanHT-12 v4 BeadChip array (ILLUMINA) by the Core Unit for DNA technologies of the University Hospital Leipzig. The R package limma was used to perform preprocessing (i.e., background correction and quantile normalization) and differential gene expression analyses[40]. Fold changes were $\log_2$-transformed and *p*-values were adjusted for multiple testing using Benjamini-Hochberg procedure (False Discovery Rate, FDR).

qRT-PCR

TaqMan quantitative real-time polymerase chain reaction (qRT-PCR) was performed as previously described[39] using the QuantStudio3 Real-Time PCR System (Applied Biosystems®) and using the qPCR™ Mastermix Plus - Low ROX (Eurogentec Deutschland GmbH) or the Takyon™ Low Rox Probe Mastermix dTTP Blue (Eurogentec Deutschland GmbH). Gene expression was quantified using a standard curve of serial dilutions from a linearized plasmid containing the target sequence or from a reference sample. Gene expressions were normalized to the expression of β-actin and TATA-box-binding protein. Table S4 lists all sequences of primers and probes and TaqMan™ Gene Expression Assays (Thermo Fisher Scientific Inc.) used for qRT-PCRs.

5’RACE PCR

5’ Rapid amplification of cDNA-ends and PCR (5’RACE PCR) was performed using the SMARTer™ RACE cDNA Amplification Kit (Clontech Laboratories, Inc.) using the agouti-signaling protein (*ASIP)*-specific primer 5’-TTGAGGCTGAGCACGCGGCAGGAGCAGG-3’ and the nested *ASIP*-specific primer 5’-CTGCGGAAGAAGCGGCACTGGCAGGAGG-3’. As template, RNA from peripheral blood leukocytes from the patient was used.

RNA sequencing and transcript analyses

RNA was isolated from SVF cells of the patient and control children 1-4 as well as from peripheral blood mononuclear cells of the patient and control 9 using TRI REAGENT™ (Sigma-Aldrich) according to the manufacturer's instructions. RNA quantity was measured with a spectrometer (Nanodrop ND 1000), and RNA quality was analyzed on the Agilent 2100 bioanalyzer using the RNA 6000 Nano Chip (Agilent Technologies, USA). We only included RNA samples with an RIN value above 8. Indexed cDNA libraries were generated using TruSeq RNA Sample Preparation kits v2 (Illumina, USA) according to the manufacturer's protocol. The average library size was 300 bp as determined on the Agilent 2100 Bioanalyzer with DNA 1000 Chips. The libraries were sequenced on the Illumina HiScanSQ Sequencing System (Fa Macrogen Europe).

Reads were mapped to the reference *human* genome (GRCh38.p13 (Genome Reference Consortium Human Build 38), INSDC Assembly GCA_000001405.28, Dec 2013) using Tophat[41]. Reads which did not map uniquely to a genome position were excluded. After indexing with samtools[42] the mapped reads were assembled to transcripts and quantified by StringTie[43,44]. For Tophat, we used the 'default' parameters which are commonly used in most studies. StringTie parameters 'read coverage' (-c), 'transcript length' (-m) and 'bases on both sides of a junction a spliced read has to cover' (-a) were set to minimal values in order to avoid missing transcripts and generating a bias. The parameter 'fraction of most abundant transcript at one locus' (-f) was lowered from default (0.01) to 0 since correction for artifacts and incompletely processed mRNA with a 1% cutoff was performed after the comparative analysis. For all other StringTie parameters default values were used. Assembled transcripts were inspected with the Integrated Genome Viewer (Broad Institute)[45,46] and samples showing a visible 3' bias due to oligo-dT/poly-A primer selection were not included.

Due to small sizes of the exons of *ITCH* and *ASIP* coverage analyses of single exons were not possible. Instead, a *de novo* assembly of *ITCH* and *ASIP* transcripts was performed using StringTie. Three novel transcript variants occurred containing only the first 2 annotated exons of *ITCH*. The fragments per kilo base per million mapped reads for these variants and also of the *ASIP* transcripts were compared between the patient and the controls in both tissues.

Trio whole genome sequencing, panel sequencing and copy number variation analyses

Trio whole genome sequencing and bioinformatics analyses were performed at the DRESDEN-concept Genome Center. After ultrasonic shearing of 800 ng gDNA (LE220, Covaris) the DNA library preparation was done using the Kapa HyperPlus Kit (Roche) according the manufacturer's instructions. After ligation with uniquely dual indexed adapters (IDT), non-ligated adaptors were removed by adding XP beads (Beckmann Coulter) in a ratio of 1:0.9. The DNA libraries were then size selected with XP beads to an average insert size of 300 bp and quantified by qPCR (LightCycler 480, Roche) and the Fragment Analyzer (Agilent). Libraries were sequenced paired end 2 x 150 bp to a coverage > 38x on a NovaSeq

6000 (ILLUMINA). Bioinformatic analysis was performed using the ILLUMINA DRAGEN pipeline (07.021.595.3.7.5).

The TruSight One Sequencing panel has been performed after enrichment with Nextera DNA Flex Pre-Enrichment LibraryPrep and Enrichment, IDT for ILLUMINA Nextera UD Indexes and the NextSeq 500/550 High Output v2 kit (300 cycles) using the ILLUMINA NextSeq 500/550. Data were analysed using the software Varvis and Varfeed (Limbus, Rostock).

Molecular karyotyping of genomic DNA has been performed by array comparative genomic hybridization using the Infinium CytoSNP-850K v1.2 BeadChip (ILLUMINA) and analysed using BlueFuse Multi (version 4.4).

Generation of luciferase reporter vectors and expression constructs

DNA sequences were cloned and propagated according to the TOPO® TA Cloning® Kit, Dual Promoter protocol and confirmed by sequencing by the Core Unit for DNA technologies of the University of Leipzig. The *ITCH-ASIP* gDNA fusion sequence was cloned from gDNA from the patient using the *ITCH-ASIP* fusion primers indicated in Table S4.

The promoter sequence of *ITCH* (NM031483.7) (2,868 bp) was cloned from gDNA from the patient using the primers (5' in 3'): forward ACTGGAGCTCGAAGTGGTTTTGAAAGTACTTTGCT and reverse ACTGCTCGAGAAAGCGCAGGCGCCTGAGCGCG. *ASIP* (NM001672.2) and *ITCH-ASIP* mRNA sequences were cloned from cDNA from SVF cells of the patient using primers

ASIP: forward ACTGCCATGGGCCTCCTGGGATGGATGTCACCC,

reverse ACTGTCTAGATGGGGGCGCTCAGCAGTTGAGGC and

ITCH-ASIP: forward ACTGCCATGGAGCTGTGGTCGGGGCTCGGGAC,

reverse ACTGTCTAGATGGGGGCGCTCAGCAGTTGAGGC.

For luciferase assays the *ITCH* promotor was inserted upstream the luciferase reporter gene into the pGL3-Basic vector using the restriction enzymes *Sac*I and *Xho*I.

For generation of modified pGL3-Basic expression vectors containing the *ASIP* or the *ITCH-ASIP* coding sequence under control of *ITCH* or no promoter, the luciferase reporter gene was cut out of the pGL3-Basic vector using *Nco*I and *Xba*I and the cloned mRNA sequences were inserted. Subsequently, the promoter sequence of *ITCH* was inserted into those vectors using the restriction enzymes *Sac*I and *Xho*I.

A second independent expression vector containing the coding sequence of *ASIP* fused to the 5'-UTR of *ITCH* under control of the *ITCH* promoter (2.8 kbp upstream of transcription start) was generated by Taconic Bioscience GmbH, Germany as shown in Figure S5.

Luciferase assay

For luciferase reporter assays, 500,000 HEK293 cells were seeded per well (6-well dish plate) and were co-transfected 24 hours post-seeding with 1 µg of pGL3-Basic plasmids containing the firefly luciferase reporter under control of a 2,868 bp *ITCH* promoter sequence or no promoter, and 50 ng of pRL-CMV control plasmid containing the luciferase gene from *Renilla reniformis* using 3 µL Fugene HD transfection reagent (Promega). Luciferase activities were measured using the Dual-Luciferase Reporter Assay System (Promega) according to the manufacturer's protocol 48 hours post-transfection using a CLARIOstar plate reader (BMG Labtech). Experiments were performed in technical duplicates. For normalization, the sum of firefly luciferase signal was divided by the sum of *Renilla* luciferase signal.

Inhibition of secretory pathway in SVF cells for immunoblotting

For inhibition of the classical secretory pathway, 800,000 SVF cells were seeded on 15-cm plates. When grown to 95% confluency, cells were treated for 24 hours with 15 mL FBS-free media containing penicillin, streptomycin, 0.1% bovine serum albumin (Invitrogen) 5 µg/mL brefeldin A (solved in dimethyl sulfoxide (DMSO), BioLegend), and 2 µM monensin (solved in 70% ethanol, BioLegend). Medium containing the same volume of DMSO and 70% ethanol was used as a negative control.

Patient-derived induced pluripotent stem cell (iPSC) generation and pluripotency analyses

The generation of induced pluripotent stem cells from SVF cells isolated from adipose tissue of the patient and two control patients, 1 and 10, was performed by the iPSC Core Facility, Institute of Stem Cell Research, Helmholtz Zentrum München, Neuherberg, Germany and pluripotency was confirmed by staining of OCT4, SOX2, LIN28 and NANOG[47]. The iPSCs were cultivated on Geltrex (Thermo Fisher Scientific) coated cell culture plates in mTeSR™1 medium (Stem Cell™ Technologies) at 37 °C and 5% CO_2.

Characterization of the pluripotency of patient-derived induced pluripotent stem cells (iPSCs) was performed as monolayers by directed differentiation into the ectodermal[48], mesodermal[49] and endodermal[50] germ layers for a period of 5 days and subsequent qRT-PCR analyses of marker genes for each of the germ layers[47]. Relative expression levels were calculated using the Delta-Delta Ct method normalized to β-actin.

Immunoblotting

For analysis of ASIP protein secretion in SVF cells from the patient and controls, the cells and the conditioned medium were harvested after 24 hours of incubation with the medium containing the secretory pathways inhibitors brefeldin A and monensin or the control medium.

For analysis of ASIP protein expression, 600,000 HEK cells were seeded per 6-well dish and were transfected 24 hours later with 2 µg plasmid using 8 µL using Fugene HD transfection reagent (Promega)

per well. Medium was changed 24 hours post-transfection. Cells and supernatants were harvested 48 hours post-medium change for immunoblotting.

For the analysis of ASIP protein expression and secretion in the generated iPSC lines, the cells were grown in 6-well-plates to 100% confluence before medium was changed to 1 ml knockout DMEM with 1x MEM NEAA, 1x β–mercaptoethanol, 0.1% BSA (Albumin bovine Fraction V, Protease-free, Serva, Heidelberg, GER), 100 units penicillin and 0.1 mg/mL streptomycin, 2 mM Glutamin. After 24 hours, cells and supernatants were collected for immunoblotting

Conditioned medium was centrifuged for 5 minutes at 800 x g and the supernatant was lyophilized and re-suspended in H_2O for receiving 10x concentrated conditioned medium. Cells were lysed in RIPA lysis buffer (50 mM Tris pH 7.5, 150 mM NaCl, 1% Triton X-100, 0.1% sodium dodecyl sulphate, with cOmplete™Mini Protease Inhibitor Cocktail Tablets (Roche, Sigma-Aldrich GmbH) with additional break up via QiaShredder Homogenizer Columns (Qiagen). Protein concentration of cell lysates was measured using the Pierce™ BCA Protein Assay Kit (Thermo Fisher Scientific). Equal amounts of protein or conditioned medium were resolved by 12% or 15% sodium dodecyl sulphate-polyacrylamide gel electrophoresis and ASIP was detected using an anti-ASIP antibody (PA5-77052, Invitrogen). Equal loading was confirmed by detection of β-actin using an anti-β-actin antibody (ab8227, Abcam).

CHO-K1 cell culture, transfection and ALPHAScreen cAMP assay

Chinese hamster ovary cell line CHO-K1 (ATCC CCL-61™) were obtained from ATCC and maintained at 37 °C in a humidified 5 % CO_2 incubator. CHO-K1 cells were grown in Dulbecco's Modified Eagle Medium: Nutrient Mixture F-12 (DMEM/F12) supplemented with 10 % fetal bovine serum (FBS), 100 U/ml penicillin and 100 µg/ml streptomycin. Cells were split into 25 cm^2-cell culture flasks (0.9 x 10^6 cells/flask) and the following day transfected with plasmid (total amount of DNA: 3 µg) and Lipofectamine 2000 (Thermo Fisher Scientific). Plasmids encoding human MC1R[51], human MC4R[52] and empty vector pcDps have previously been described.

One day after transfection cells were split into 96-well plates (2 x 10^4 cells/well) and 16 hours prior to the experiment, cells were serum-starved. cAMP content of cell extracts was determined by a non-radioactive assay based on the ALPHAScreen (Perkin Elmer) technology according as previously described[53]. In brief, stimulation with various α-MSH (Sigma Aldrich) concentrations in absence or presence of 100 nM ASIP (R&D systems) or with various concentrations of ASIP alone were performed 48 h after transfection. Reactions were stopped by aspiration of media and cells were lysed in 20 µl of lysis buffer containing 1 mM 3-isobutyl-1-methylxanthine (IBMX). From each well 5 µl of lysate were transferred to a 384-well plate. Acceptor beads and donor beads were added according to the manufacturers' protocol. Cyclic AMP accumulation data were analyzed using GraphPad Prism version 8.4.3.

Screening for patients with *ASIP* mutations

20 patients with obesity and red hair color, who were previously suspected for mutations in the proopiomelanocortin gene, and one patient with obesity and red hair color from the outpatient clinic of the Hospital for Children and Adolescents, University of Leipzig were screened for genomic *ITCH-ASIP* fusion. The patients were recruited at the Freie Universität Berlin, Humboldt-Universität zu Berlin, Institute for Experimental Pediatric Endocrinology, Berlin, Germany (mean age: 9.4 years, female: n = 13, male: n = 7). This analysis was approved by the local ethical committee (EA2/131/11). gDNA copy numbers of the *ITCH-ASIP* fusion sequence were quantified using SYBR green qRT-PCR using the Maxima SYBR Green/ROX qPCR Master Mix (2x) (Thermo Fisher Scientific) and the *ITCH-ASIP* fusion primers (Table S4) with an input of 2 ng gDNA per reaction.

The parents of the patient were analyzed for the patient-specific tandem duplication using the *ITCH-ASIP* fusion primers (Table S4).

Copy numbers were normalized to copy numbers of β-actin. On each plate, samples from the patient and the father were carried along as a positive control.

Statistical analyses

Statistical analyses were performed using Student's t-test (two-sided) in GraphPad Prism 6 (GraphPad Software, San Diego, CA). *P*-values <0.05 were considered statistically significant.

Declarations

Declaration of interests

The authors declare no conflict of interests.

Data availability

The datasets generated during and/or analysed during the current study are available from the corresponding author on reasonable request.

Contributors

AK was the project principal investigator and led the design of the study, established the project and funding, and supervised experiments, analyses, and data interpretation. AK assumes responsibility for the completeness and integrity of the data and the fidelity of the report. WK contributed to project management, data interpretation, and discussion of manuscript. EK, RS, MH, AH, RAJ, AKü, YHT, TS, WR, EZ, KL, and AK performed and supervised experiments, performed clinical assessments and data analysis and interpretation, and drafted the manuscript. PK provided the cohort samples for mutation screening. MB edited the manuscript. All authors contributed to the interpretation of study findings and had the opportunity to review and revise the final manuscript.

Acknowledgements and funding

We thank all the children and parents who participated in the study, all the physicians and technical assistants who helped with the study, and Udo Stenzel for the bioinformatic transcript analyses. We would also like to thank Ejona Rusha and Dr. Anna Pertek from the iPSC Core Facility, Institute of Stem Cell Research, Helmholtz Zentrum München for generating the iPSCs. This work was supported by the German Research Foundation (DFG) for the Clinical Research Center “Obesity Mechanisms” SFB1052/CRC1052 (No 209933838) projects C05 to AK, C09 to AK and KL, and KO3512/3-1 to AK and EZ, and by the German Diabetes Association (DDG) to AK. RS was funded by the joint Clinician Scientist Program of the Medical Faculty and the Helmholtz Institute for Metabolic, Obesity, and Vascular Research of the Helmholtz Zentrum München at the University of Leipzig. The funders of the study had no role in the study design, in the collection, analysis, and interpretation of data, or in the writing of the report.

References

1. Bouchard C. Genetics of obesity: What we have learned over decades of research. Obesity 2021;29:802–20.
2. van der Klaauw AA, Farooqi IS. The hunger genes: pathways to obesity. Cell 2015;161:119–32.
3. Lotta LA, Mokrosiński J, Mendes de Oliveira E, et al. Human gain-of-function MC4R variants show signaling bias and protect against obesity. Cell 2019;177:597–607.e9.
4. Wabitsch M, Pridzun L, Ranke M, et al. Measurement of immunofunctional leptin to detect and monitor patients with functional leptin deficiency. Eur J Endocrinol 2017;176:315–22.
5. Marenne G, Hendricks AE, Perdikari A, et al. Exome sequencing identifies genes and gene sets contributing to severe childhood obesity, linking PHIP variants to repressed POMC transcription. Cell Metab 2020;31:1107-19.e12.
6. Clément K, van den Akker E, Argente J, et al. Efficacy and safety of setmelanotide, an MC4R agonist, in individuals with severe obesity due to LEPR or POMC deficiency: single-arm, open-label, multicentre, phase 3 trials. Lancet Diabetes Endocrinol 2020;8:960–70.
7. Ericson MD, Freeman KT, Schnell SM, Fleming KA, Haskell-Luevano C. Structure-activity relationship studies on a macrocyclic agouti-related protein (AGRP) scaffold reveal agouti signaling protein (ASP) residue substitutions maintain melanocortin-4 receptor antagonist potency and result in inverse agonist pharmacology at the melanocortin-5 receptor. J Med Chem 2017;60:8103–14.
8. Klebig ML, Wilkinson JE, Geisler JG, Woychik RP. Ectopic expression of the agouti gene in transgenic mice causes obesity, features of type II diabetes, and yellow fur. Proc Natl Acad Sci U S A 1995;92:4728–32.
9. Duhl DM, Vrieling H, Miller KA, Wolff GL, Barsh GS. Neomorphic agouti mutations in obese yellow mice. Nat Genet 1994;8:59–65.
10. Moussa NM, Claycombe KJ. The yellow mouse obesity syndrome and mechanisms of agouti-induced obesity. Obesity research 1999;7:506–14.

11. Miltenberger RJ, Mynatt RL, Wilkinson JE, Woychik RP. The role of the agouti gene in the yellow obese syndrome. J Nutr 1997;127:1902S-7S.
12. Morgan MD, Pairo-Castineira E, Rawlik K, et al. Genome-wide study of hair colour in UK Biobank explains most of the SNP heritability. Nat Commun 2018;9:5271.
13. Kempf E, Vogel M, Vogel T, et al. Dynamic alterations in linear growth and endocrine parameters in children with obesity and height reference values. EClinicalMedicine.
14. Kwon HY, Bultman SJ, Löffler C, et al. Molecular structure and chromosomal mapping of the human homolog of the agouti gene. Proc Natl Acad Sci U S A 1994;91:9760–4.
15. Yang Y-K, Ollmann MM, Wilson BD, et al. Effects of recombinant agouti-signaling protein on melanocortin action. Mol Endocrinol 1997;11:274–80.
16. Patel MP, Cribb Fabersunne CS, Yang YK, Kaelin CB, Barsh GS, Millhauser GL. Loop-swapped chimeras of the agouti-related protein and the agouti signaling protein identify contacts required for melanocortin 1 receptor selectivity and antagonism. Journal of molecular biology 2010;404:45–55.
17. He Z, Gao Y, Lieu L, et al. Direct and indirect effects of liraglutide on hypothalamic POMC and NPY/AgRP neurons - Implications for energy balance and glucose control. Mol Metab 2019;28:120–34.
18. Voisey J, Van Daal A. Agouti: from Mouse to Man, from Skin to Fat. Pigment Cell Res 2002;15:10–8.
19. Small CJ, Liu YL, Stanley SA, et al. Chronic CNS administration of Agouti-related protein (Agrp) reduces energy expenditure. Int J Obes Relat Metab Disord 2003;27:530–3.
20. Tang-Christensen M, Vrang N, Ortmann S, Bidlingmaier M, Horvath TL, Tschöp M. Central administration of ghrelin and agouti-related protein (83–132) increases food intake and decreases spontaneous locomotor activity in rats. Endocrinology 2004;145:4645–52.
21. Cavalcanti-de-Albuquerque JP, Bober J, Zimmer MR, Dietrich MO. Regulation of substrate utilization and adiposity by Agrp neurons. Nat Commun 2019;10:311.
22. Lubrano-Berthelier C, Dubern B, Lacorte JM, et al. Melanocortin 4 receptor mutations in a large cohort of severely obese adults: prevalence, functional classification, genotype-phenotype relationship, and lack of association with binge eating. J Clin Endocrinol Metab 2006;91:1811–8.
23. Mynatt RL, Stephens JM. Regulation of PPARgamma and obesity by agouti/melanocortin signaling in adipocytes. Annals of the New York Academy of Sciences 2003;994:141–6.
24. Schnabl K, Westermeier J, Li Y, Klingenspor M. Opposing Actions of Adrenocorticotropic Hormone and Glucocorticoids on UCP1-Mediated Respiration in Brown Adipocytes. Front Physiol 2018;9:1931.
25. Nakayama K, Ishida T. Alu-mediated 100-kb deletion in the primate genome: the loss of the agouti signaling protein gene in the lesser apes. Genome Res 2006;16:485–90.
26. Chandramohan B, Renieri C, La Manna V, La Terza A. The alpaca agouti gene: genomic locus, transcripts and causative mutations of eumelanic and pheomelanic coat color. Gene 2013;521:303–10.

27. Girardot M, Guibert S, Laforet MP, Gallard Y, Larroque H, Oulmouden A. The insertion of a full-length Bos taurus LINE element is responsible for a transcriptional deregulation of the Normande Agouti gene. Pigment Cell Res 2006;19:346–55.
28. Norris BJ, Whan VA. A gene duplication affecting expression of the ovine ASIP gene is responsible for white and black sheep. Genome Res 2008;18:1282–93.
29. Robic A, Morisson M, Leroux S, et al. Two new structural mutations in the 5' region of the ASIP gene cause diluted feather color phenotypes in Japanese quail. Genet Sel Evol 2019;51:12.
30. Landgraf K, Rockstroh D, Wagner IV, et al. Evidence of early alterations in adipose tissue biology and function and its association with obesity-related inflammation and insulin resistance in children. Diabetes 2015;64:1249–61.
31. Kromeyer-Hauschild K, Wabitsch M, Kunze D, et al. Percentiles of body mass index in children and adolescents evaluated from different regional German studies. Monatsschr Kinderh 2001;149:807–18.
32. Evidence-based (S3) guideline of the Working Group on Childhood and Adolescent Obesity (AGA) of the German Obesity Society (DAG) and the German Society of Pediatrics and Adolescent Medicine (DGKJ). 2019. (Accessed February 8th, 2021, at https://awmf.org/leitlinien/detail/ll/050-002.html.)
33. Hilbert A, Tuschen-Caffier, B. Eating Disorder Examination-Questionnaire: Deutschsprachige Übersetzung. Münster: Verlag für Psychotherapie.; 2006.
34. Fairburn CG. Cognitive behavior therapy and aating disorders. New York: Guilford Publications; 2008.
35. Hilbert A, de Zwaan M, Braehler E. How frequent are eating disturbances in the population? Norms of the eating disorder examination-questionnaire. PloS one 2012;7:e29125.
36. Nagl M, Hilbert A, de Zwaan M, Braehler E, Kersting A. The German version of the Dutch Eating Behavior Questionnaire: psychometric properties, measurement invariance, and population-based norms. PloS one 2016;11:e0162510.
37. Landgraf K, Klöting N, Gericke M, et al. The obesity-susceptibility gene TMEM18 promotes adipogenesis through activation of PPARG. Cell Rep 2020;33.
38. Doubling Time Computing. 2006 at http://www.doubling-time.com/compute.php.)
39. Bernhard F, Landgraf K, Klöting N, et al. Functional relevance of genes implicated by obesity genome-wide association study signals for human adipocyte biology. Diabetologia 2013;56:311–22.
40. Smyth G, Thorne N, Wettenhall J. limma: Linear models for microarray data user's guide. Bioinformatics and computational biology solutions using R and bioconductor2011.
41. Langmead B, Trapnell C, Pop M, Salzberg SL. Ultrafast and memory-efficient alignment of short DNA sequences to the human genome. Genome Biol 2009;10:R25.
42. Li H, Handsaker B, Wysoker A, et al. The Sequence Alignment/Map format and SAMtools. Bioinformatics 2009;25:2078–9.
43. Pertea M, Kim D, Pertea GM, Leek JT, Salzberg SL. Transcript-level expression analysis of RNA-seq experiments with HISAT, StringTie and Ballgown. Nat Protoc 2016;11:1650–67.

44. Pertea M, Pertea GM, Antonescu CM, Chang T-C, Mendell JT, Salzberg SL. StringTie enables improved reconstruction of a transcriptome from RNA-seq reads. Nat Biotechnol 2015;33:290–5.
45. Robinson JT, Thorvaldsdóttir H, Winckler W, et al. Integrative genomics viewer. Nat Biotechnol 2011;29:24–6.
46. Thorvaldsdóttir H, Robinson JT, Mesirov JP. Integrative Genomics Viewer (IGV): high-performance genomics data visualization and exploration. Briefings in bioinformatics 2013;14:178–92.
47. Eberherr AC, Maaske A, Wolf C, et al. Rescue of STAT3 Function in Hyper-IgE Syndrome Using Adenine Base Editing. The CRISPR journal 2021;4:178–90.
48. Shi Y, Kirwan P, Livesey FJ. Directed differentiation of human pluripotent stem cells to cerebral cortex neurons and neural networks. Nature Protocols 2012;7:1836–46.
49. Borchin B, Chen J, Barberi T. Derivation and FACS-mediated purification of PAX3+/PAX7 + skeletal muscle precursors from human pluripotent stem cells. Stem cell reports 2013;1:620–31.
50. Ori C, Ansari M, Angelidis I, Theis FJ, Schiller HB, Drukker M. Single cell trajectory analysis of human pluripotent stem cells differentiating towards lung and hepatocyte progenitors. bioRxiv 2021:2021.02.23.432413.
51. Lalueza-Fox C, Rompler H, Caramelli D, et al. A melanocortin 1 receptor allele suggests varying pigmentation among Neanderthals. Science 2007;318:1453–5.
52. Stäubert C, Tarnow P, Brumm H, et al. Evolutionary aspects in evaluating mutations in the melanocortin 4 receptor. Endocrinology 2007;148:4642–8.
53. Peters A, Rabe P, Krumbholz P, et al. Natural biased signaling of hydroxycarboxylic acid receptor 3 and G protein-coupled receptor 84. Cell Commun Signal 2020;18:31.
54. Bussler S, Vogel M, Pietzner D, et al. New pediatric percentiles of liver enzyme serum levels (alanine aminotransferase, aspartate aminotransferase, γ-glutamyltransferase): Effects of age, sex, body mass index, and pubertal stage. Hepatology 2018;68:1319–30.

Figures

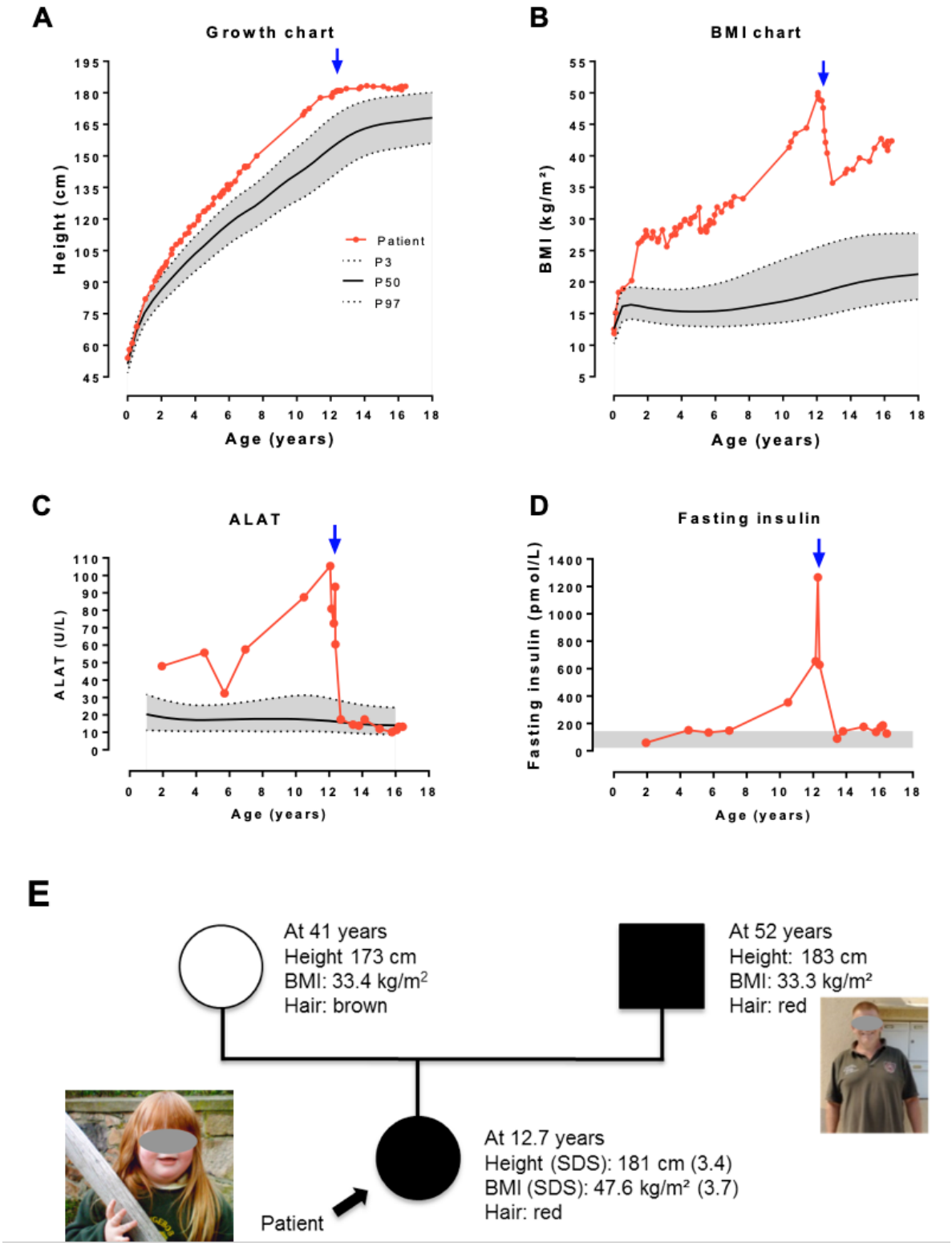

Figure 1

Clinical characteristics of the patient and her family

(A) Height and (B) body mass index (BMI) of the patient during childhood and adolescence compared with the 3rd (P3), 50th (P50), and 97th (P97) percentiles for girls according to Kromeyer-Hauschild et al.[31] are presented. Data from the patient until the age of 2 years were corrected for gestational age. (C) Serum

levels of alanine aminotransferase (ALAT) are indicated with the 3rd (P3), 50th (P50), and 97th (P97) percentile according to Bussler et al.[54] and (D) fasting insulin levels are related to the reference range of the local hospital lab (20–144 pmol/L). The red arrow marks the time at which the patient had bariatric surgery at the age of 12.4 years. (E) The pedigree of the family: females are presented as circles and the father as a square. Individuals carrying the *ASIP* tandem duplication are presented as black symbols, the open symbol represents the mother, who does not carry the mutation. The patient investigated in this study is marked with a black arrow. Phenotype data and photos are given next to the symbols.

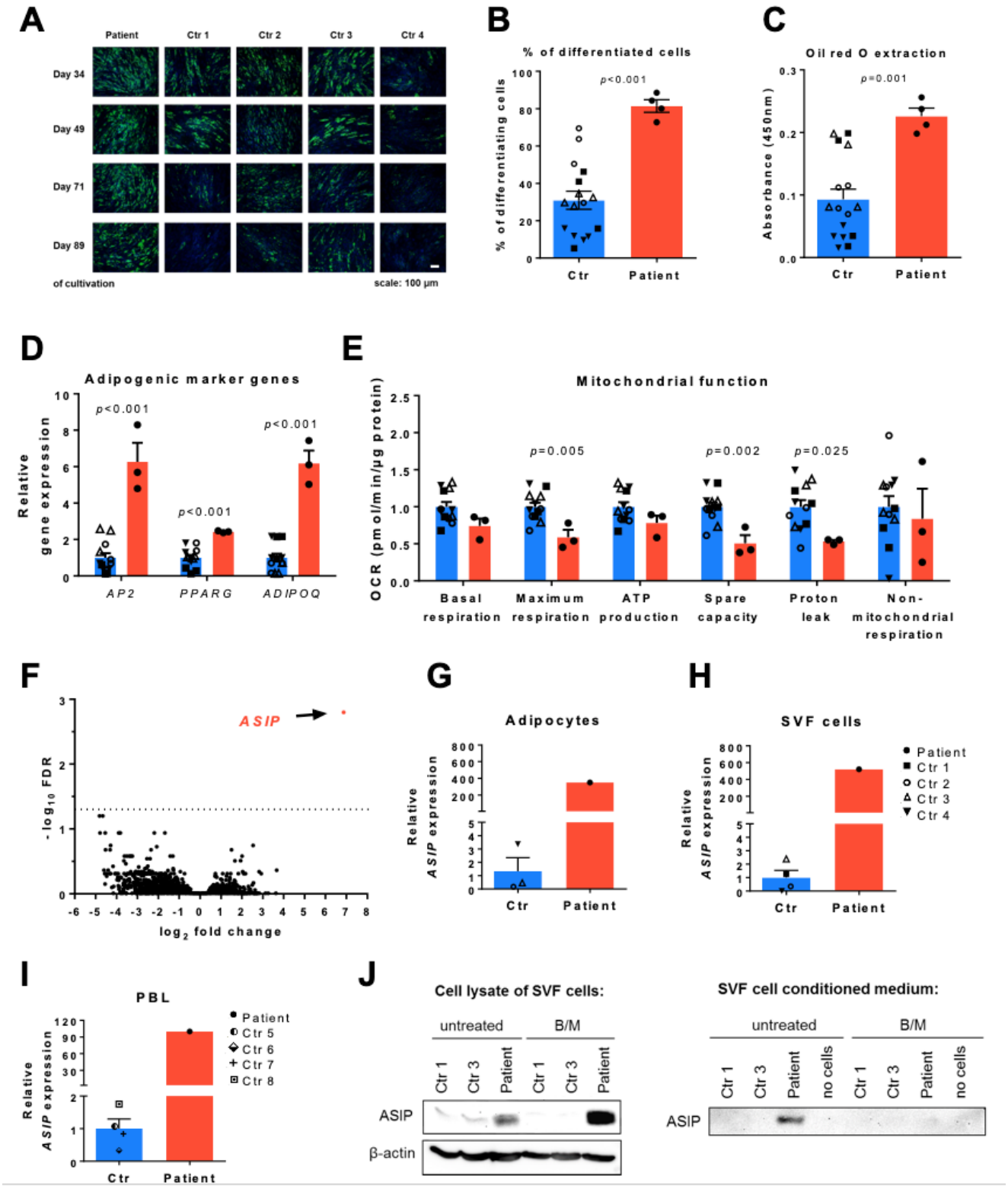

Figure 2

Identification of ectopic *ASIP* expression in the patient

(A) At different times of cultivation (day 34, 49, 71, and 89) subcutaneous stromal vascular fraction (SVF) cells from the patient and control (Ctr) children (n=4) were differentiated into adipocytes (3 technical replicates per time point). Nuclei were stained with Hoechst (blue), lipids were stained with Nile red

(green), and (B) the percentage of differentiated cells was determined by cell counting. (C) Adipogenic capacity was quantified using oil red O. (D) Relative expression of the adipogenic marker genes adipocyte protein 2 (*AP2*), peroxisome proliferator-activated receptor gamma (*PPARG*), and adiponectin (*ADIPOQ*) in differentiated SVF cells is shown. The experiment was performed in 3 replicates (cells seeded for differentiation at days 65, 83, and 98 of cultivation). (E) Mitochondrial function of SVF cells from the patient and controls was assessed using the Seahorse Mito Stress Test Kit. (F) Differentially expressed genes between undifferentiated SVF cells from the patient and control children 1–4 are presented as the $\log_2$ of the fold change of gene expression across the $-\log_{10}$ of the false discovery rate (FDR). Agouti-signaling protein (*ASIP*) gene expression levels are shown for (G) adipocytes, (H) SVF cells, and (I) peripheral blood leukocytes (PBL). As PBL RNA samples from control children 1–4 were not available, measurements were performed in control children 5–8 (Supplementary Appendix, Table S1). (J) ASIP protein was detected by immunoblotting in cell lysates and conditioned medium from untreated and brefeldin A- and monensin (B/M)-treated SVF cells from the patient and two control children, 1 and 3. Gene expression data were normalized to the expression of β-actin and TATA-box-binding protein and are presented as fold change in relation to the mean (with standard error) of the controls. All bars from controls are shown in blue and from the patient in red. *P*-values derived using Student's t-test are given.

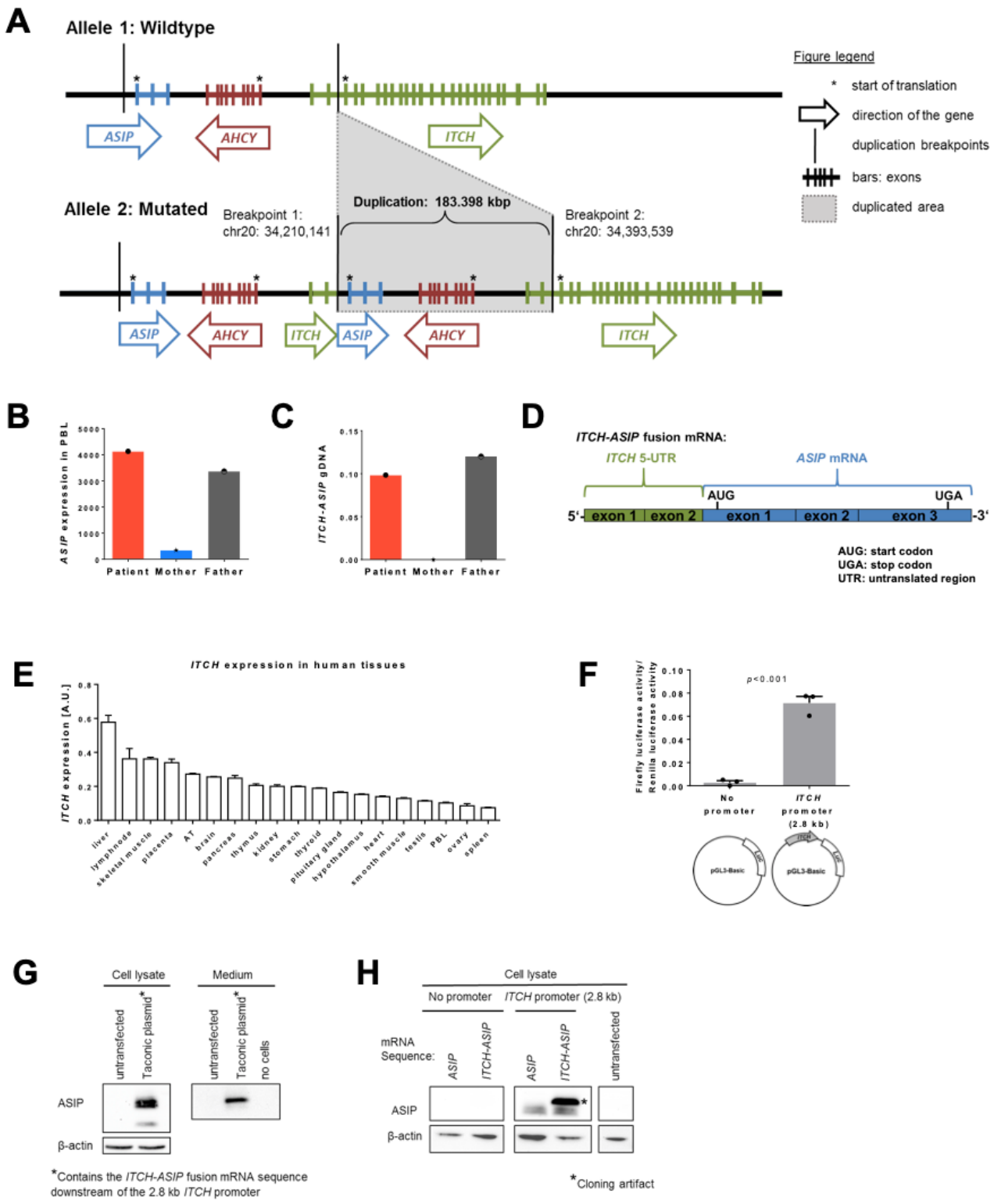

Figure 3

A heterozygous tandem duplication in the *ASIP* locus inherited from the father leads to ubiquitous *ASIP* expression

(A) Scheme of the wild type allele and the 183-kbp tandem duplication at the agouti-signaling protein (*ASIP*), adenosylhomocysteinase (*AHCY)*, and itchy E3 ubiquitin protein ligase (*ITCH)* locus found in the

patient. Locations of the duplication breakpoints are presented according to the Dec. 2013 GRCh38/hg38 assembly. (B) *ASIP* gene expression in peripheral blood leukocytes (PBL) in the patient, the mother, and the father normalized to β-actin and TATA-box-binding protein. (C) Quantification of the copy number of breakpoint-specific *ITCH-ASIP* fusion genomic DNA (gDNA) in the patient, the mother, and the father, normalized to the respective copy number of β-actin gDNA. (D) Scheme of the *ITCH-ASIP* fusion mRNA generated from the duplication identified by 5¢ rapid amplification of cDNA ends and polymerase chain reaction (5¢-RACE PCR). (E) Gene expression of *ITCH* in human tissues normalized to expression of β-actin and TATA-box-binding protein. Data is presented as mean with standard error of 3 technical replicates. AT, adipose tissue; PBL, peripheral blood leukocytes. (F) Luciferase assays in HEK293 cells transfected with the pGL3-Basic vector without a promoter or containing a 2.8-kbp *ITCH* promoter sequence upstream of the luciferase (Luc) reporter gene. Firefly luciferase activity was normalized to *Renilla* luciferase activity. The statistical significance of the difference was assessed using Student's t-test. (G) Immunoblot of ASIP in cell lysates and conditioned medium from untransfected HEK293 cells or cells transfected with the Taconic expression plasmid containing the *ITCH-ASIP* fusion mRNA sequence under control of the 2.8-kbp *ITCH* promoter. (H) Immunoblot of ASIP in cell lysates and conditioned medium from HEK293 cells transfected with modified pGL3-Basic plasmids containing either the physiological *ASIP* coding sequence or the *ITCH-ASIP* fusion mRNA sequence downstream of no promoter or the *ITCH* promoter.

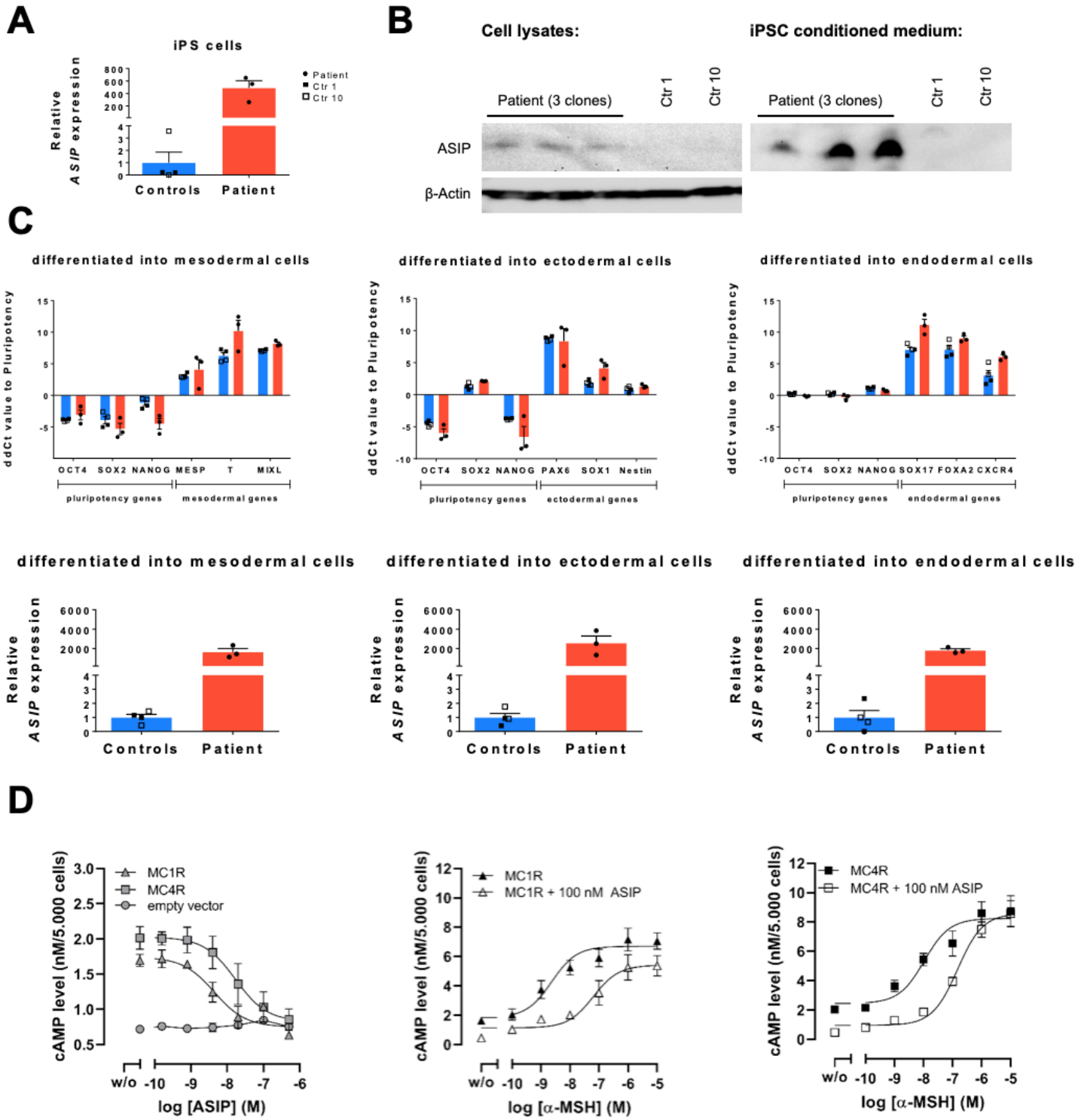

Figure 4

Ectopic *ASIP* expression is present in patient-derived iPSCs and persists during differentiation in all three germ layers.

(A) *ASIP* gene expression levels are shown for SVF cell-derived iPSCs from three clones of the patient and two clones from each of the control (Ctr) children, 1 and 10. (B) ASIP protein was detected by immunoblotting in cell lysates and conditioned medium from untreated iPS cells from the patient and the

two control children, 1 and 10. (C) Patient-derived iPSCs and iPSCs of two control children were differentiated to the three germ layers. Successful differentiation was confirmed by down-regulation of the pluripotency markers *OCT4*, *SOX2* and *NANOG* and the up-regulation of germ layer-specific markers (*MESP*, *T* and *MIXL* for mesoderm; *PAX6*, *SOX1* and *Nestin* for ectoderm; *SOX17*, *FOXA2* and *CXCR4* for endoderm) determined by quantitative real-time PCR. Ectopic *ASIP* expression in the patient-derived iPSCs persists during differentiation into each of the three germ layers. Results of two consecutive passages of three clones from the patient and 2 clones from each of the control children are shown. *ASIP* expression data were normalized to the expression of β-actin and TATA-box-binding protein and are presented as fold change in relation to the mean (with standard error) of the controls. Relative expression levels of marker genes for the three germ layer were calculated using the Delta-Delta Ct method normalized to β-actin. Bars from controls are shown in blue, bars from the patient in red. (D) Inverse agonistic activity of ASIP in absence and presence of α-MSH at human MC1R and MC4R. Basal cAMP levels were concentration-dependently decreased in presence of increasing concentrations of ASIP (MC1R IC_{50} = 4.4 nM; MC4R IC_{50} = 16.9 nM). α-MSH stimulates both MC1R (EC_{50} = 2.3 nM) and MC4R (EC_{50} = 10.6 nM). Presence of 100 nM ASIP lower the potency of α-MSH at MC1R (EC_{50} = 65 nM) and at MC4R to (EC_{50} = 149 nM). Data is shown as mean ± SEM of n = 3 independent experiments each carried out in duplicates.

Supplementary Files

This is a list of supplementary files associated with this preprint. Click to download.

- 220310ASIPNatMedSupplementaryInformationclean.docx
- ASIPnreditorialpolicychecklist.pdf
- ASIPnrreportingsummary.pdf
- KempfetalCAREchecklist.pdf